



## Measurement of apparent attenuation in seismic sections by using waveform synthetics

Osama El Badri and Igor B. Morozov

University of Saskatchewan, ose767@mail.usask.ca, igor.morozov@usask.ca

### Summary

Measurement of attenuation effects on seismic waveforms is a key part of analysing and correcting seismic records for attenuation effects. However, in such analysis, true physical properties causing seismic attenuation are not always clearly differentiated from “apparent”, or measured quantities. The usually-measured  $Q$  and the associated cumulative attenuation  $t^*$  are such apparent quantities. These quantities can be frequency-dependent and different for different attenuation mechanisms, such as viscoelastic, pore-fluid flows, solid viscosity, or wave-front focusing. The apparent  $Q$  and  $t^*$  also vary for propagating P and S waves, reflections, effects of thin layering, multiples, or surface waves.

In this study, we measure the detailed distance- and time-dependent  $t^*(x,t)$  within seismic sections. Several types of apparent  $Q^{-1}(x,t)$  sections can be derived from these  $t^*$  sections. Because such detailed  $t^*$  cannot be modeled directly, we propose measuring it by using synthetic waveform modeling conducted for identical geometries and subsurface structures. In one of these sections, we model the elastic wavefield, and the second section contains all attenuation effects. In order to produce the apparent  $t^*$  including the dispersion (phase shift) effects, we measure the time-variant spectral ratios between the attenuated and elastic synthetic sections.

The resulting “sections” of  $t^*(x,t)$  and  $Q^{-1}(x,t)$  attributes can be utilized in two ways. First, they can be compared to the attenuation models used for forward modeling (viscoelastic  $Q$  in the present examples). Second, accurate attenuation-compensation of the synthetic and real data can be carried out by using these  $t^*(x,t)$  sections.

### Introduction

Measurements of attenuation and velocity dispersion effects in refraction and reflection seismic data are important in several ways in seismic data analysis. Zones of increased attenuation are often used for characterizing hydrocarbons or for identifying small-scale heterogeneity within the subsurface, and knowledge of dispersion can be used for accurate correlation of seismic sections to acoustic logs and performing well ties. Alternatively, attenuation and dispersion effects often reduce the quality of reflection seismic sections, which need to be corrected during data processing. Quantitative knowledge of attenuation effects is also necessary for implementing numerical seismic modeling.

In all of the above applications, it is necessary to clearly define the meanings of the measured “attenuation” and “dispersion” parameters, to select the measurement procedures, and to evaluate their accuracy. First, it is important to note that all practically used measures of attenuation are “apparent” quantities, i.e. quantities measured in the data but not necessarily

present within rock (Morozov and Baharvand Ahmadi, 2015). The key property of such kind is the complex-valued  $t^*$ , defined from the relation between the spectra of an attenuated ( $W$ ) and elastic ( $W_{el}$ ) wavefields at the same point  $x$  and time  $t$  in a seismic section:

$$W(\omega | x, t) = e^{-\pi f t^*(x, t)} W_{el}(\omega | x, t) , \quad (1)$$

where  $f$  is the frequency. From this relation, several useful types of inverse “Q-factors” can be derived, for example:

$$Q_{\text{vertical}}^{-1} \equiv \frac{\partial t^*}{\partial t} , \quad Q_{\text{ray}}^{-1} \equiv \frac{dt^*}{dt} \Bigg|_{\text{along ray path } x(t)} , \quad \text{or} \quad Q_{\text{average}}^{-1} \equiv \frac{t^*}{t} . \quad (2)$$

The function  $t^*(x, t)$  represents a useful complex-valued attribute of a seismic section. For modeling and attenuation corrections of seismic sections, knowledge of this attribute is sufficient (Morozov et al., 2018). By contrast, for interpretation, “local” attributes such as  $Q^{-1}$  are required. Note that  $t^*(x, t)$  is a well-defined property obtained by directly comparing two wavefields (eq. (1)), but  $Q^{-1}$  only exists for certain waves and within certain theoretical models, such as a body wave traveling along a certain path in the second eq. (2). For example, if point  $(x, t)$  corresponds to a multiple in a reflection record, the  $t^*(x, t)$  would still be meaningful but  $Q^{-1}(x, t)$  difficult to define.

In the following, we measure the  $t^*(x, t)$  from synthetic seismic reflection sections and further examine its properties. Two important applications of such measurements could consist in obtaining detailed measurements of the  $Q^{-1}$  by relations (2) and direct attenuation-compensation filtering (deriving  $W_{el}(x, t)$  from the  $W(x, t)$ ; Hale, 1981; Wang, 2008) by using inverse eq. (1).

## Method

Usually, the  $Q$  and  $t^*$  are modeled by using ray tracing, for example by assuming vertically-propagating waves in the case of reflection seismic data. In the present approach, we used the full-waveform forward modeling in order to measure not only the (assumed)  $Q$  values of the subsurface but the complete attenuation including variations of geometric spreading, scattering and multiples, and potentially other non- $Q$  type physical factors such as solid viscosity (Morozov et al., 2018).

In order to obtain a  $t^*(x, t)$  section suitable for detailed testing, we generated a three-component synthetic dataset for a 1-D anelastic subsurface structure with  $Q = 30$  by using the “reflectivity” method (Fuchs and Müller, 1971) (Figure 1). This method accounts for all finite-frequency effects,

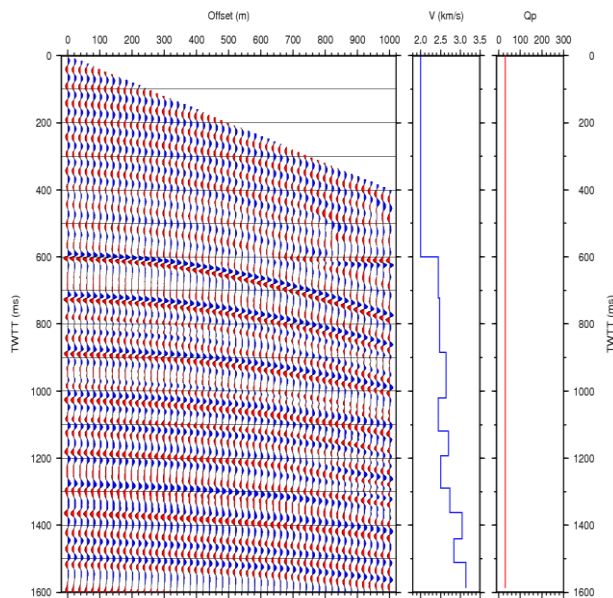


Figure 1. Synthetic dataset containing only the major layering

multiples, and AVO effects. Note that although the viscoelastic “Q” is not the only and likely not the best description of anelasticity in Earth media, this is currently the only modeling method available, and we use it for this testing. Our goal will be to treat the dataset in Figure 1 as “field” data and use it for measuring the  $t^*$  and  $Q^{-1}$  for the major reflectors, and to compare these attributes to the known  $Q^{-1}$  of the subsurface.

To produce a  $t^*(x,t)$  section with coverage between and above the major reflections, we further generated two additional sections with additional weak reflectivity included at all depths within the model (Figures 2 and 3). One of these synthetic wavefields was modeled with  $Q^{-1} = 0$  within the subsurface (Figure 2), and the second synthetic included all effects of attenuation (Figure 3). By performing time-variant deconvolution of these “anelastic” and “elastic” sections, inverse of eq. (1)), the desired  $t^*(x,t)$  is obtained. Figure 4 shows the  $Q_{\text{vertical}}^{-1}$  (eqs. (2)) derived from this  $t^*$  map. Note that for major reflectors, reasonable values close to the modeled  $Q^{-1} = 1/30$  are obtained. At the same time, significant variations and deviations from the constant expected  $Q^{-1}$  are also seen.

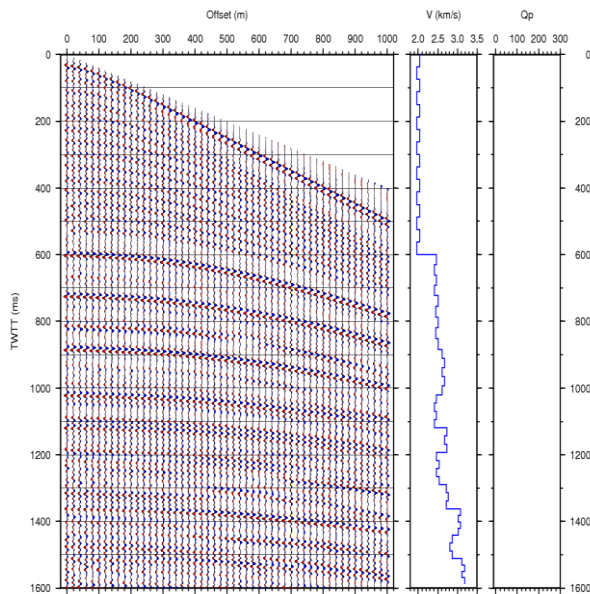


Figure 2. Attenuation-free synthetic seismic data modeled in a 1-D, elastic layered structure

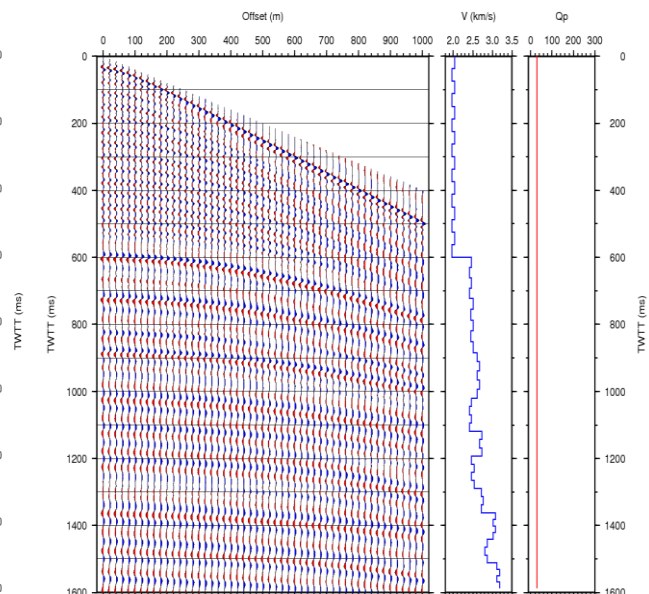


Figure 3. Synthetic seismic traces modeled in the same layered structure as in Figure 2 but with attenuation ( $QP = 30$ ; panel on the right)

## Results

Figure 5 illustrates the  $Q^{-1}$  values measured at three different reflectors which are derived from  $t^*$  by relations (2). The upper plot of figure 5 shows the  $Q^{-1}$  measured at 600 ms. As we can see in this plot, for most of the locations that the measured  $Q^{-1}$  is close to the modeled  $Q^{-1}$  ( $1/30$ ). However, the locations where  $Q^{-1}$  value is less than zero, we could not measure  $Q^{-1}$  value that is close to the modeled  $Q^{-1}$  value due to the effects of thin layering and multiples. In the middle plot in Figure 5 (860-ms reflector), the inverted  $Q^{-1}$  is close to the model  $Q^{-1}$  value for

offsets below 600 m, and in most other areas, the  $Q^{-1}$  values oscillate with peak values generally corresponding to the expected  $Q^{-1} = 1/30$ . Also note the measured  $Q^{-1}$  values dropping below zero at several offset ranges (Figure 5). These inaccuracies of the measured  $Q^{-1}$  and deviations from the model  $Q^{-1}$  should be due to the effects of multiples, thin layering, P- and S-wave mode conversions, and interferences with the direct S and surface waves that seem to be noticeable in Figure 4. In Figure 4, these zones are clearly seen by the dark blue color. In the bottom plot in

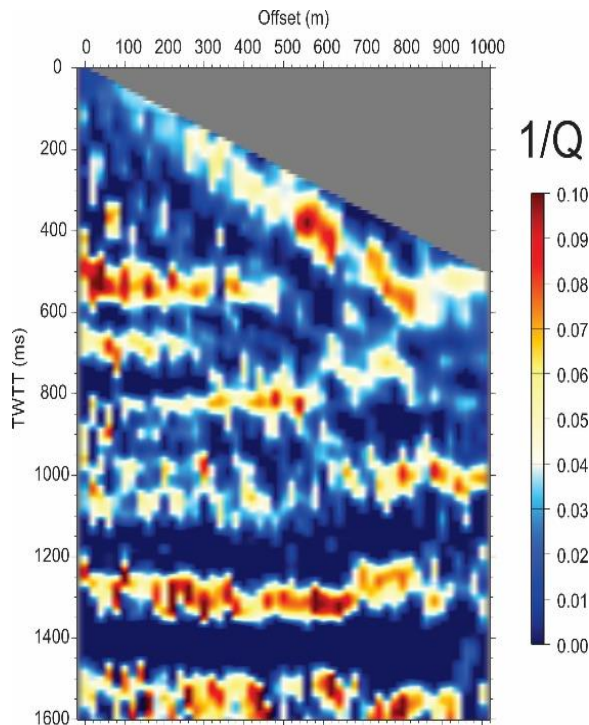


Figure 4.  $Q^{-1}$  attribute (eq. 2) derived from NMO-corrected synthetic sections in Figures 2 and 3.

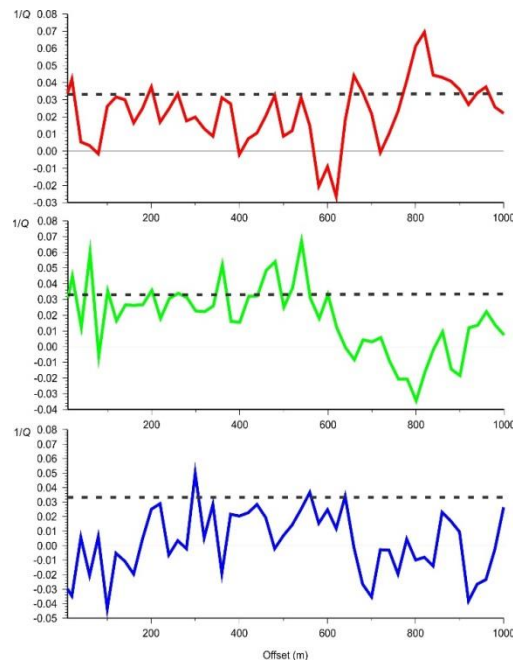


Figure 5.  $Q^{-1}$  attribute (eq. 2) measured at three different reflector times (600,860, and1360 ms).

Figure 5 corresponding to the deepest 1360-ms reflector, the measured  $Q^{-1}$  is below the actual  $Q^{-1}$  value for most of the offset range and is below zero for many offset intervals. Thus, detailed measurements of  $Q^{-1}(x,t)$  are sensitive to numerous effects of wave interference. At the same time, the larger values of  $Q^{-1}(x,t)$  (Figures 4 and 5) tend to correspond to the correct  $Q^{-1}$ .

## Conclusions

Time-variant deconvolution of synthetic records generated in anelastic and elastic models gives a general and powerful approach to measuring all realistic effects of attenuation in seismic records. In contrast to the traditional Q models, the new approach uses full-waveform forward modeling and allows measuring the complete attenuation for reflections, multiples, and other types of waves. The attenuation attributes  $t^*$  and  $Q^{-1}$  are extracted in the forms of record sections that can be used for interpretation and attenuation-compensation.

## **Acknowledgements**

The work by Osama El Badri was supported by Libyan Education Ministry.

## **References**

- Fuchs, K. and G. Müller, 1971. Computation of synthetic seismograms with the reflectivity method and comparison with observations, *Geophysical Journal International*, 23, 417–433.
- Hale, D., 1981. An inverse- $Q$  filter. *Stanford Exploration Project*, 28(1), 289-298.
- Morozov, I.B. and A. Baharvand Ahmadi, 2015. Taxonomy of  $Q$ , *Geophysics* 80, No. 1, T41–T49.
- Morozov, I. B., M. Haiba, & W. Deng., 2018. Inverse attenuation filtering, *Geophysics*, 83, No. 2. V135–V147, doi: 10.1190/GEO2016-0211.1
- Wang, Y. 2008, *Seismic inverse Q filtering*: Blackwell, ISBN 978-1-4051-8540-0.